Coupling Conversion of *n*-Hexane and CO over an HZSM-5 Zeolite: Tuning the H/C Balance and Achieving High Aromatic Selectivity

Changcheng Wei, Qijun Yu, Jinzhe Li, and Zhongmin Liu*

Read Online

ACCESS | Metrics & More | Article Recommendations | SI Supporting Information

ABSTRACT: The coupling conversion of *n*-hexane (a model compound of naphtha) and CO was conducted over an HZSM-5 zeolite catalyst. A significant increase in the aromatic selectivity and dramatic decrease in the alkane selectivity were simultaneously achieved by adjusting the H/C ratio of the reactants. Under suitable conditions, the aromatic selectivity was 80%, which far exceeds the theoretical value for the conversion of only *n*-hexane over HZSM-5. Detailed studies revealed that the high aromatic selectivity originated from the direct incorporation of CO into the products. Different characterization methods were used to elucidate the coupling reaction mechanism. Important reaction intermediates, such as acyl groups and oxygenates (substituted cyclopentenones), were detected. Isotope labeling studies revealed that oxygenates were formed by ^{13}CO incorporation into alkyl species, and they could transform into aromatic products. Based on these findings, a plausible reaction mechanism of the coupling transformation was proposed. The coupling effect between *n*-hexane and CO over HZSM-5 demonstrated in this work contradicts the traditional view that metal catalysts are indispensable for the highly selective conversion of naphtha to aromatics. This type of coupling reaction might have great potential for industrial applications, considering the large existing supply capacities of CO and alkanes.

Coupling conversion of n-hexane and CO over HZSM-5

KEYWORDS: *coupling, n-hexane, carbon monoxide, HZSM-5, aromatics*
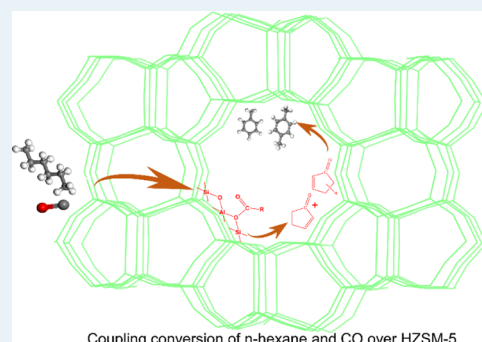
1. INTRODUCTION

Naphtha is one of the most important oil-based chemical feedstocks that is widely used for the production of basic chemicals such as light olefins and aromatics.[1] The conversion of naphtha into these relatively hydrogen-deficient substances is thermodynamically unfavorable with strongly endothermic characteristics; therefore, either a high reaction temperature or a large amount of heat supply is needed to realize economically efficient processes. The production of light olefins from naphtha, the so-called naphtha steam cracking process, is aided by steam at extremely high temperatures (>800 °C) and generates a lot of methane as a byproduct (methane/ethene ≈ 1/2). Aromatics are produced by the catalytic reforming of naphtha in the presence of hydrogen over noble metal catalysts (Pt/Al_2O_3) at 450−550 °C.[2] These catalysts are very sensitive to impurities, such as sulfur and nitrogen compounds, and the hydrotreatment of naphtha is required. In this process, the straight-chain paraffins of naphtha are easily isomerized to produce branched paraffins, but it is difficult to transform them into aromatics. Increasing the naphtha utilization efficiency and reducing the energy consumption of the processes are still challenges for new technology development. The main problem might possibly be the limitations stemming from the large difference in the H/C ratios of naphtha and the target products.

Alternatively, chemicals can be produced from coal or natural gas by C1 chemistry using a syngas platform. Syngas, a mixture of carbon monoxide (CO) and hydrogen (H_2), can serve as a feedstock for the synthesis of liquid fuels (mainly paraffins) by the Fischer−Tropsch process and the synthesis of chemicals such as methanol and C_2-oxygenates, which could also be used as intermediates for further transformations. These reactions are mostly thermodynamically favorable with exothermic characteristics. Methanol-to-olefin technology has already been developed and employed in many coal-to-olefin plants.[3] Researchers are also developing methanol-to-aromatics technologies for aromatics production. Most recently, Bao and Pan et al. reported that syngas can be directly transformed into aromatics or olefins over OX-ZEO (oxide-zeolite) bifunctional catalysts.[4]

The activation of CO, one of the main components of syngas, over noble metals or metal−organic complexes has been widely studied in C1 chemistry. It should be noted that

carbonylation reactions of CO with oxygenates and hydrocarbons also occur over acid catalysts, although only a few publications in the broader area of alkane carbonylation are available. It was reported that superacidic HF/SbF$_5$ and/or CF$_3$SO$_3$H/SbF$_5$ could catalyze alkane carbonylation to form carboxylic acids, aldehydes, or ketones.[5] Stepanov and co-workers observed isobutane carbonylation with CO over sulfated zirconia using in situ NMR characterization.[6] Alkane carbonylation over a Zn-ZSM-5 zeolite was also observed by solid-state NMR.[7] In another related report, signals corresponding to carboxylic acids and alkanes were observed by solid-state NMR during the coreaction of CO, H$_2$O, and propane or isobutane over an HZSM-5 zeolite.[8] The results proved that alkanes could react with CO to generate carboxylic acids, aldehydes, or ketones under certain conditions. However, the product yields of these reactions were very low.

CO conversion with dimethyl ether to generate methyl acetate over HMOR was first reported by Fujimoto in 1984.[9] Iglesia[10] and Shen et al.[11] further investigated this reaction over many zeolite catalysts in detail, and a higher CO conversion and methyl acetate yield were obtained over an H-mordenite zeolite. Bell and co-workers reported that CO carbonylation with dimethoxymethane occurred even under mild reaction conditions.[12] tert-Butyl alcohol or isobutylene reacted with CO to form trimethylacetic acid over HZSM-5, as reported by Stepanov et al.,[13] and methanol carbonylation through a Koch-type reaction over zeolite catalysts was also reported.[14] Recently, the coupling of methanol with CO over HZSM-5 to obtain aromatics with high selectivity was reported by our research laboratory.[15]

Zeolites are widely used in the refining and petrochemical industries[16] and have found many applications in the transformation of hydrocarbons, such as catalytic cracking, isomerization, alkylation, transalkylation, aromatization, and so forth. The catalytic cracking of naphtha over zeolites has been widely studied and is considered to be an alternative technology to steam cracking due to its lower energy consumption and higher propene/ethene ratio at lower temperatures; in particular, the HZSM-5 zeolite is thought to be an efficient and promising catalyst due to its unique channel system. To enhance naphtha conversion and supply heat to the cracking reaction, the coupling conversion of n-hexane (a model compound of naphtha) with methanol was investigated over an HZSM-5 catalyst,[17] and the reaction exhibited higher initial conversion rates and a lower activation energy compared with n-hexane cracking. Methyl acetate was also found to exhibit synergistic effects in its coupling conversion with n-hexane over zeolites;[18] the n-hexane conversion improved, and the initial temperature of n-hexane cracking was reduced. C$_4$ hydrocarbons were also used in coupling reactions with methanol by Nowak and co-workers.[19]

These data for the activation and conversion of CO over acidic zeolite catalysts without the assistance of a noble metal, especially the fact that CO could react with dimethyl ether and dimethoxymethane via a carbonylation reaction under mild reaction conditions, suggest that CO could be active at higher reaction temperatures in a zeolite catalytic reaction system. This hypothesis leads to the idea of simultaneously converting alkanes from naphtha and CO from syngas in one process, that is, the coupling reaction of naphtha and CO, which is very attractive from the viewpoint of heat balance, H/C balance, and potential industrial applications and is also advantageous for addressing the complementary interests of the petrochem-

ical and coal/natural gas chemical industries, because naphtha is from the petrochemical industry and CO is abundant in the coal/natural gas chemical industry. According to the effective hydrogen index (EHI) proposed by Chen et al.,[20] saturated alkanes are compounds with a "net" hydrogen-to-carbon ratio (i.e., EHI > 1). In contrast, CO is a "hydrogen-deficient" compound (i.e., EHI < 1) and therefore might have synergistic effects on alkane conversion due to EHI matching.

In this study, the coreaction of n-hexane (a model compound of naphtha) and CO over an HZSM-5 zeolite was systematically investigated, and high aromatic selectivity could be achieved under suitable reaction conditions. Using in situ characterization observations and isotope labeling experiments, the effects of the coupling reaction of n-hexane and CO were demonstrated, and a reaction mechanism was proposed.

2. EXPERIMENTAL SECTION

2.1. Catalyst and Reaction Tests. The HZSM-5 zeolite was purchased from NanKai University. The samples were calcined at 600 °C for 5 h to remove the template, and then, they were tableted, crushed, and sieved to 40−60 mesh for the reaction tests. Carbon monoxide (89.9%, containing 10.1% Ar as an internal standard) and propene (5.0%, He as the balance) were purchased from Dalian Special Gases Co., Ltd. Dichloromethane (>99.5%) and n-hexane (>99.5%) were purchased from Dalian Bono Biochemical Reagent Factory.

The catalytic reactions were performed in a stainless steel fixed-bed reactor lined with 6 mm of quartz tube. Typically, 0.4 g of the catalyst was packed in a quartz tube and activated at 550 °C for 60 min in a helium stream before reaction. n-Hexane was introduced into the catalyst bed by passing a carrier gas (He or CO) into a stainless steel saturator maintained at 29 °C. The reaction contact time was adjusted by changing the catalyst weight. The CO partial pressure was changed while maintaining a constant total pressure with He as the balance. For comparison, the coupling conversion of propene and CO was also conducted at different CO partial pressures (up to 0.95 MPa) and a constant propene mass space velocity (0.1 h^{-1}) and reaction contact time (~2 s).

The effluent products were analyzed by an on-line gas chromatograph (Agilent 7890A) equipped with an Agilent HP-1 capillary column connected to a flame ionization detector and a TDX-01 packed column connected to a thermal conductivity detector (TCD).

The CO conversion (Con$_{CO}$) and CO$_2$ selectivity (Sel$_{CO_2}$) were calculated based on the CO concentration difference between the inlet (CO$_{inlet}$) and outlet (CO$_{outlet}$), and CO$_2$ was detected at the outlet (CO$_{2outlet}$) by GC using Ar as an internal standard.

$$\text{Con}_{CO} = \frac{CO_{inlet} - CO_{outlet}}{CO_{inlet}} \times 100\%$$

$$\text{Sel}_{CO_2} = \frac{CO_{2outlet}}{CO_{inlet} - CO_{outlet}} \times 100\%$$

n-Hexane conversions (Con$_{n-hexane}$) were calculated using the following formula based on the consistency of the carbon number between the inlet and outlet streams. Hexane$_{inlet}$ and hexane$_{outlet}$ represent the carbon mole fractions of n-hexane at the inlet and outlet, respectively.
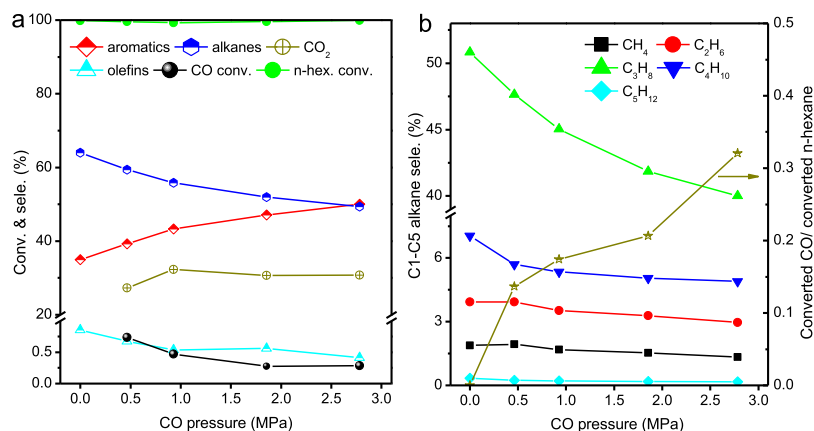
Figure 1. Effects of the CO partial pressure on the coupling reaction over HZSM-5: (a) conversion and selectivity, (b) detailed alkane selectivities for $C_1 - C_5$ and the molar ratio of converted CO to converted *n*-hexane. Reaction conditions: T = 400 °C, *n*-hexane WHSV = 0.17 $g \cdot g^{-1} h^{-1}$, (CO + $Ar_{internal\ standard}$ + $He_{balance}$)/*n*-hexane = 120, P = 3.0 MPa, TOS = 3 h.

$$\text{Con}_{n\text{-hexane}} = \frac{\text{hexane}_{\text{inlet}} - \text{hexane}_{\text{outlet}}}{\text{hexane}_{\text{inlet}}} \times 100\%$$

The selectivity of component C_nH_m ($\text{Sel}_{C_nH_m}$) in the hydrocarbon products was calculated using the following equation

$$\text{Sel}_{C_nH_m} = \frac{C_nH_{m_{\text{outlet}}}}{\sum C_nH_{m_{\text{outlet}}}} \times 100\%$$

where $C_nH_{m_{\text{outlet}}}$ represents the carbon mole fraction of product C_nH_m at the outlet. $\sum C_nH_{m_{\text{outlet}}}$ represents the sum of the carbon mole fractions of all the hydrocarbon products (not including Hexane$_{\text{outlet}}$) at the outlet.

The H/C ratio of the products was calculated using the following equation

$$H_{\text{all products}}/C_{\text{all products}} = \frac{\sum_1^n \frac{X_{C_nH_m}}{M_{C_nH_m}} \times m}{\sum_1^n \frac{X_{C_nH_m}}{M_{C_nH_m}} \times n}$$

where $X_{C_nH_m}$ and $M_{C_nH_m}$ represent the mass percentage and molecular weight of C_nH_m, respectively, in the products.

2.2. Catalyst Characterization. The HZSM-5 zeolite morphology was characterized by scanning electron microscopy at 2.0 kV using a Hitachi SU8020 instrument. The ratio of silica to alumina was determined by XRF using a PANalytical AXIOS spectrometer. The Brunauer−Emmett−Teller surface area and pore volume of the sample were obtained by nitrogen sorption experiments on a Micromeritics ASAP-2020 analyzer at 77 K after the sample was degassed at 350 °C under vacuum. Ammonia temperature-programmed desorption (NH₃-TPD) experiments were conducted on a Micromeritics AutoChem 2920 instrument equipped with a TCD detector. First, 0.2 g of the catalyst sample was loaded into a quartz tube, pretreated at 650 °C in an He flow for 30 min, and then cooled to 100 °C and saturated with NH₃. After the sample was pretreated with He gas to remove physically adsorbed ammonia, desorption was performed from 100 to 650 °C at a heating rate of 10 °C/min in He gas.

Catalyst acidities were characterized by Fourier transform infrared spectroscopy with adsorption of pyridine (Py-FTIR) on a Bruker Tensor 27 spectrometer with an MCT detector. Typically, HZSM-5 (20 mg) was pressed into a self-supporting

wafer and placed in a quartz cell. The samples were pretreated at 400 °C for 30 min under vacuum and cooled to 150 °C. The spectrum of HZSM-5 without pyridine perturbations was collected. Afterward, the IR cell was saturated with pyridine and subsequently evacuated for 30 min to remove physically adsorbed pyridine. Then, the spectrum of Py-FTIR was collected from 4000 to 1000 cm^{-1} by averaging 64 scans with a resolution of 4 cm^{-1}.

2.3. In situ DRIFT Spectroscopy Study. In situ DRIFT spectra were collected on a Bruker Tensor 27 FTIR spectrometer equipped with a diffuse reflectance attachment and MCT detector. The catalyst powder was loaded into the diffuse reflectance infrared cell with a ZnSe window that could withstand high temperatures and pressures. After the catalyst was calcined at 500 °C for 1 h under a 30 mL/min (at STP) N_2 stream and cooled to 170 °C, the cell was filled with an *n*-hexane saturated stream (25 °C) carried by 30 mL/min N_2 for 0.5 h and subsequently swept by 30 mL/min N_2 for 0.5 h to remove *n*-hexane from the gas phase. Then, a CO stream (30 mL/min) was introduced into the cell, and the in situ DRIFT spectra were collected as the temperature was increased from 170 to 400 °C at a constant rate of 10 °C/min. All of the spectra were recorded with 16 scans at a resolution of 4 cm^{-1}. The IR difference spectra were obtained by subtracting the spectra of the HZSM-5 zeolite framework from the collected spectra at the corresponding temperatures.

2.4. Isotope Tracing Experiments. These experiments were conducted using the same apparatus as the catalytic tests with ^{13}CO and ^{12}C hexane as the reactants. *n*-Hexane was carried by passing 5 mL/min He gas to the saturator at 15 °C and mixing with 30 mL/min ^{13}CO before introduction into the reactor. The reaction temperature was 250 °C at atmospheric pressure. The gas-phase products were collected by CH_2Cl_2 absorption and analyzed by gas chromatography−mass spectrometry (GC−MS) to determine the isotopic distribution. After 10 min of time on stream, the catalyst was removed from the reactor and quenched by liquid nitrogen in a Teflon tube. The species retained in the catalyst were analyzed and identified by the method introduced by Guisnet,[21] in which 0.1 g of the recovered catalyst was dissolved in 1 mL of a 20% HF solution, and the organic species were extracted by 0.5 mL of CH_2Cl_2 and analyzed using an Agilent 7890A/5975C GC/MSD instrument.

2.5. Switching Experiments. The switching experiments were conducted on the setup used for the catalytic tests described in Section 2.1. The reaction was performed at 500 °C and atmospheric pressure. *n*-Hexane was carried by passing 5 mL/min He gas through the saturator at 15 °C and mixing it with He (98 mL/min) before introduction into the reactor. After 80 min of reaction, the flow was switched from He (98 mL/min) to CO (98 mL/min) for another 80 min and then back to He (98 mL/min). An on-line mass spectrometer (Omnistar) was connected to the reactor outlet to monitor the water/CO/CO_2/He concentrations.

3. RESULTS AND DISCUSSION

3.1. Effects of the CO Partial Pressure on the Coupling Reaction of *n*-Hexane and CO over HZSM-5. The HZSM-5 catalyst was characterized by multiple techniques (the results are shown in Table S1, Figure S1 and Figure S2 in the Supporting Information) and demonstrated to be well crystallized with a size of 1−2 μm, surface area of 406 m²/g, and acid site concentration of 0.82 mmol/g. The catalytic behaviors at different CO partial pressures are shown in Figure 1. Apparently, CO addition improved the aromatic selectivity at a similar *n*-hexane conversion (nearly 100%). Generally, aromatics were formed from alkenes through hydrogen transfer reactions during hydrocarbon transformation over the HZSM-5 zeolite. From the viewpoint of the H/C balance, a higher aromatic selectivity means more hydrogen-rich byproducts (such as alkanes). However, with increasing CO partial pressure, the aromatic selectivity increased, whereas all of the C_1−C_5 alkane selectivities decreased (Figure 1b); in particular, the selectivity to propane decreased significantly. Meanwhile, the generation of olefins and hydrogen was very low under these reaction conditions. A comparison of the product distributions of *n*-hexane cracking in He and CO atmospheres with time on stream is presented in Figure S3. Dramatic improvements in the selectivity to toluene, xylene, and C_{9+} aromatics were also observed with decreasing alkane selectivity. These results could not be explained by the conventional aromatization of olefins through hydrogen-transfer reactions and might indicate a new aromatic generation pathway in the coupling reaction.

Although the CO conversion was always less than 1% and decreased with increasing CO partial pressure (Figure 1a), further analysis of the data revealed that the molar ratio of converted CO to converted *n*-hexane significantly increased with CO partial pressure (right *y*-axis of Figure 1b). Because *n*-hexane was completely converted, this result indicates that the amount of converted CO increased, which is consistent with previous works that showed that carbonylation rates increased with the CO partial pressure.[22]

Table 1 lists the $H_{all\ products}$/$C_{all\ products}$ ratios obtained at different CO partial pressures. The results in Table 1 clearly show that the H/C ratio of the products systematically decreased with the increasing CO partial pressure, which is consistent with the above discussions and suggests the incorporation of C from CO into the hydrocarbon products.

Table 1. $H_{all\ products}$/$C_{all\ products}$ Ratios at Different CO Partial Pressures

CO partial pressure (MPa)	0	0.5	0.9	1.9	2.8
$H_{all\ products}$/$C_{all\ products}$	2.15	2.08	2.01	1.95	1.91

Based on the results in Table 1, the general reaction equation can be expressed as

$$1CO + 0.7C_6H_{14} \rightarrow 0.7C_7H_{12} + 0.3CO_2 + 0.3H_2$$
$$+ 0.4H_2O$$
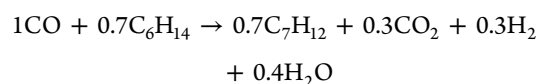
Using the molar ratio of CO to *n*-hexane in the feed, an increase of approximately 0.05 mol C per mole H was calculated, which is approximately the same as that previously calculated by product composition (0.06 mol C).

3.2. Effects of the Temperature on the Coupling Reaction of *n*-Hexane and CO over the HZSM-5 Zeolite. The effects of the reaction temperature on the coupling reaction of *n*-hexane and CO over HZSM-5 are shown in Figure 2. Clearly, the selectivity to aromatics increased almost linearly with the reaction temperature. Meanwhile, the alkane selectivity decreased significantly. An aromatic selectivity of approximately 69% and alkane selectivity of 30% were achieved at 500 °C. Because the amount of hydrogen generated under the current conditions was very small, the theoretical maximum of the aromatic selectivity (58%) for the conversion of only *n*-hexane could be calculated, assuming that *n*-hexane was completely converted to aromatics and methane (Table S2). The aromatic selectivity of 69% observed for the coupling reaction was much higher than this theoretical maximum. As shown in Figure 2b, the selectivities to propane and butane decreased with the increasing temperature, whereas the selectivities to methane and ethane increased. These results indicate that light alkanes (mainly propane and butane) could be further cracked[23] and aromatized at higher temperatures, which also improved the aromatic selectivity together with CO incorporation.

The conversions of *n*-hexane and CO increased with the reaction temperature. Specifically, the CO conversion increased rapidly at high temperatures. A control experiment conducted at 500 °C without the catalyst demonstrates that the dismutation reaction ($2CO \rightarrow C + CO_2$) had a negligible effect on the CO conversion (<0.1%) under these coupling reaction conditions.

The H/C ratios of the products at different reaction temperatures are shown in Table 2. The value of $H_{all\ products}$/$C_{all\ products}$ clearly decreased with increasing reaction temperature, which indicates that more carbon was incorporated into the products, accounting for the higher CO conversion.

3.3. Effects of the Contact Time on the Coupling Reaction of *n*-Hexane and CO over HZSM-5. The effects of the contact time on the coupling reaction are shown in Figure 3. Prolonging the contact time significantly increased the aromatic selectivity. Conversely, the olefin selectivity decreased sharply. The total alkane selectivity first increased and then decreased. Specifically, more long-chain alkanes were detected at shorter contact times. As the contact time was prolonged, more methane and ethane were detected, which might be caused by the cracking of longer alkanes. A longer contact time was beneficial for the conversion of CO and *n*-hexane, but the CO conversion increased relatively more slowly. This result indicates that CO activation on the zeolite might be the rate-determining step in the coupling conversion, which is consistent with previous works on carbonylation, such as dimethyl ether carbonylation[10,22b] and dimethoxymethane carbonylation.[12,24]

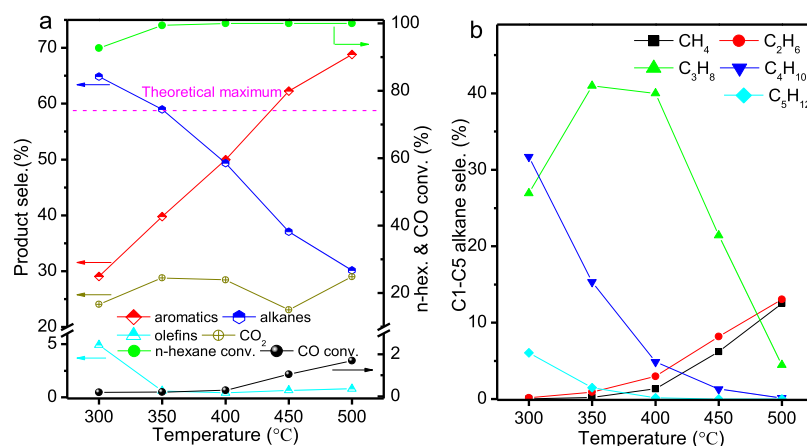Based on the above experimental results, the coupling reaction conditions were further optimized. As shown in Figure

Figure 2. Effects of the reaction temperature on the coupling reaction: (a) conversion and selectivity, (b) C_1−C_5 alkane selectivities. The theoretical maximum of the aromatic selectivity for the conversion of only *n*-hexane is marked in magenta. Reaction conditions: *n*-hexane WHSV = 0.17 g·g^{-1} h^{-1}, (CO + Ar)/*n*-hexane = 120, *P* = 3 MPa, TOS = 2.3 h.

Table 2. $H_{all\ products}$/$C_{all\ products}$ of the Products at Different Reaction Temperatures

reaction temperature (°C)	300	350	400	450	500
$H_{all\ products}$/$C_{all\ products}$	2.11	2.01	1.91	1.85	1.81

4, an aromatic selectivity of 80% and alkane selectivity of 20% were achieved over HZSM-5 at 500 °C and a CO pressure of 3 MPa when the molar ratio of (CO + Ar)/*n*-hexane was increased to 445; this high aromatic selectivity and low alkane selectivity for *n*-hexane conversion over an HZSM-5 zeolite catalyst are unprecedented and confirm the important role of the CO coupling reaction.

3.4. In situ DRIFT Study of the Coupling Reaction of *n*-Hexane and CO over HZSM-5. In situ DRIFT characterizations were performed at different temperatures, and the results are shown in Figure 5. In the O−H region, the negative bands at 3603, 3654, and 3728 cm^{-1} were attributed to the adsorption of *n*-hexane on bridging hydroxyl Si(OH)Al, Al−OH and terminal hydroxyl Si−OH groups, respectively. A broad band at 3490 cm^{-1} was assigned to the interactions of the hydrocarbons with the bridging hydroxyl groups of the zeolite.[25] The intensities of the negative band in the O−H region and the band at 3490 cm^{-1} gradually decreased, indicating that the amount of adsorbed *n*-hexane gradually

decreased with the increasing temperature. The bands at 2962, 2932 and 2873 cm^{-1} were attributed to physically adsorbed hydrocarbons, such as *n*-hexane,[26] on the zeolite, and the intensities of these bands gradually decreased as the temperature increased from 170 to 400 °C, which further confirms that the amount of adsorbed *n*-hexane gradually decreased. At the same time, new bands at 2978 and 2910 cm^{-1} assigned to the vibrations of C−H[27] appeared at 290 °C, and the former band decreased at 400 °C but later increased. These results indicate that *n*-hexane first physically adsorbed on the HZSM-5 zeolite at low temperatures (<200 °C) and then reacted with Brønsted acid sites at ∼340 °C to generate carbonium ions, which further reacted and disappeared at ∼400 °C.

More interestingly, a new band at 1680 cm^{-1} attributed to the C=O stretching mode of acyl species[28] emerged at 210 °C, which is consistent with previous MAS NMR observations of ^{13}CO and small alkane coreaction systems.[6,8,28b] These acyl species gradually disappeared when the temperature reached 340 °C, which demonstrates that carbon monoxide could react with carbonium ions to generate acyl species, and these acyl species could transform into other species at higher temperatures. In addition, a peak that might be due to the C=O stretching vibration of a carbonate phase appeared at 1431 cm^{-1} with increasing temperature.
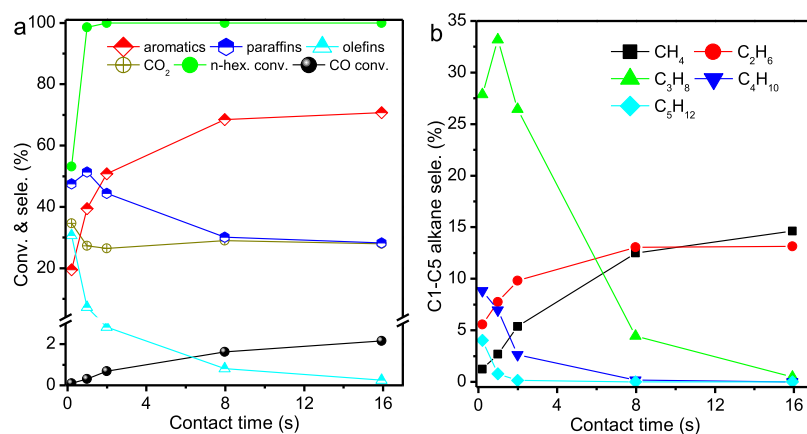

Figure 3. Effects of the contact time on the coupling reaction: (a) conversion and selectivity, (b) C_1−C_5 alkane selectivities. Reaction conditions: *n*-hexane WHSV range of 6.8 to 0.08 g·g^{-1} h^{-1}, *T* = 500 °C, (CO + Ar)/*n*-hexane = 120, *P* = 3.0 MPa, time on stream = 2.3 h.
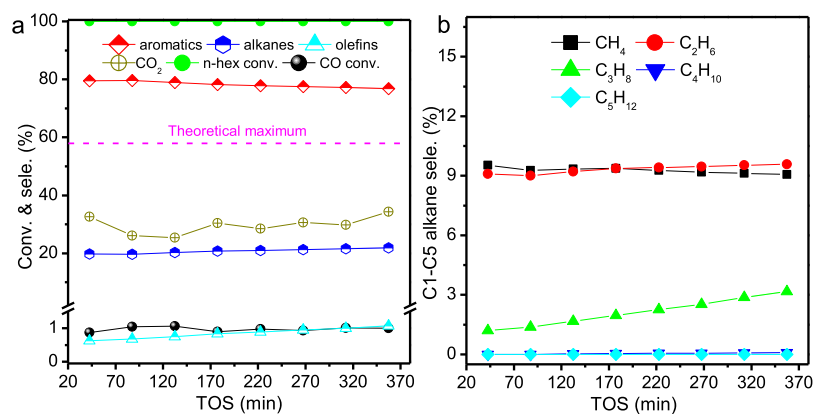
Figure 4. Coupling reaction under optimized conditions: (a) conversion and selectivity, (b) C_1–C_5 alkane selectivities. The theoretical maximum of the aromatic selectivity for the conversion of only n-hexane is marked in magenta. Reaction conditions: n-hexane WHSV = 0.05 g·g^{-1} h^{-1}, T = 500 °C, (CO + Ar)/n-hexane = 445, P = 3 MPa.
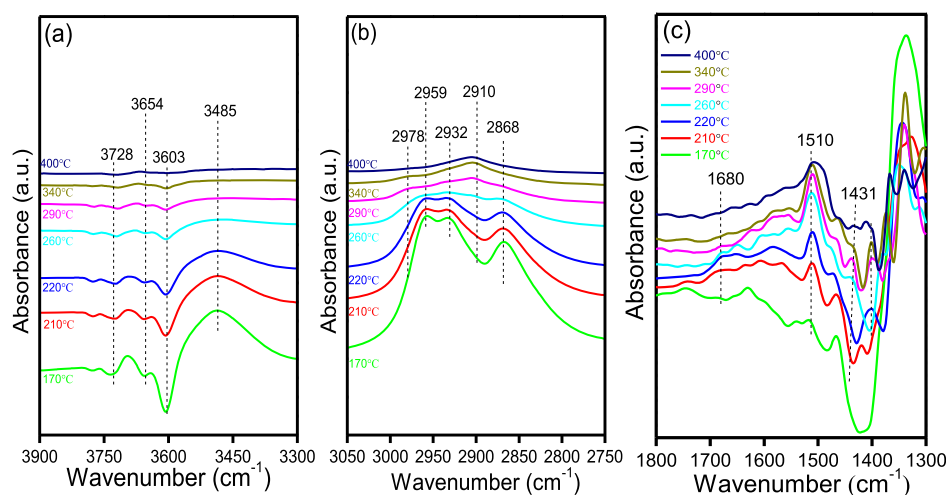

Figure 5. IR difference spectra recorded during the coupling conversion of n-hexane and CO over HZSM-5 at different temperatures: (a) O–H region, (b) H–C region, (c) region of acyl species and coke precursors.

Further studies were conducted at 200 °C (Figure S4), and after CO introduction, a band, the intensity of which increased with increasing CO time on stream, was observed at 1680 cm^{-1}. This result confirms that this band was related to CO, and it was attributed to acyl species. The band at 1510 cm^{-1} was generally attributed to alkenyl carbonium ions or coke precursors.[26b,29] The intensity of this band increased with the temperature, indicating that more carbonium ions and/or aromatics were generated by the reaction of CO with adsorbed species from n-hexane.

3.5. GC–MS Analysis of Retained Species Occluded in HZSM-5. After dissolving the catalyst in an HF solution, the retained species on the spent catalysts were extracted by CH$_2$Cl$_2$ and analyzed by GC–MS. The results are shown in Figure 6 (for retention times up to 30 min) and Figure S5 (for retention times from 30 to 58 min). Oxygenates, cyclodienes, and aromatics were detected on the catalysts at different reaction temperatures.

Methyl-substituted cyclopentadienes and cyclohexadienes were detected at lower temperatures and might be generated by the cracking of alkanes over the zeolite.[30] Very importantly, a large amount of oxygenated compounds, mainly 2-cyclopenten-1-one, 3-methyl-2-cyclopenten-1-one, 2-methyl-2-cyclopenten-1-one, 2,3-dimethyl-2-cyclopenten-1-one, and
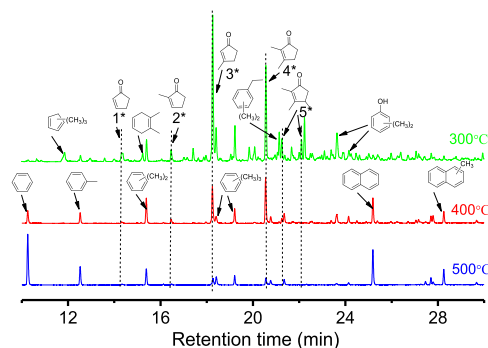

Figure 6. GC–MS results (retention times of up to 30 min) for the retained species during the coupling reaction at different temperatures. 2-Cyclopenten-1-one (1*), 2-methyl-2-cyclopenten-1-one (2*), 3-methyl-2-cyclopenten-1-one (3*), 2,3-dimethyl-2-cyclopenten-1-one (4*), and 2,3,4-trimethyl-2-cyclopenten-1-one (5*). Reaction conditions: n-hexane WHSV = 0.17 g·g^{-1} h^{-1}, (CO + Ar)/n-hexane = 120, P = 3.0 MPa. The catalysts were removed after 3 h of reaction.

2,3,4-trimethyl-2-cyclopenten-1-one (CPOs) (marked as 1*, 2*, 3*, 4*, and 5* in Figure 6), were discovered at lower temperatures. The peak intensities of these species (CPOs)
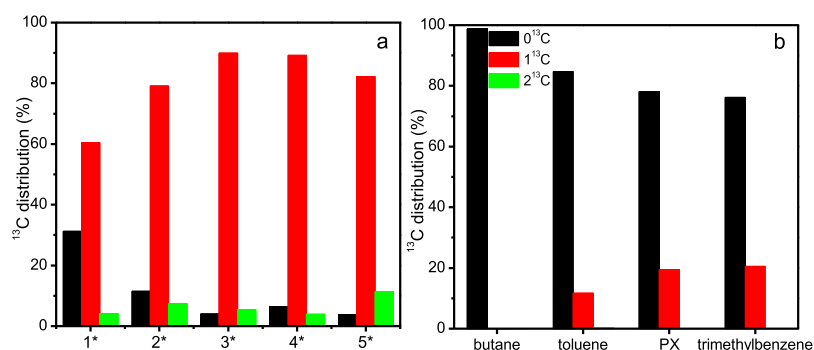
Figure 7. ^{13}C distributions of the CPOs retained on the catalyst (a) and the products in the effluent (b) during the coupling reaction of *n*-hexane and ^{13}CO.

were very strong at 300 °C and decreased dramatically as the reaction temperature increased. Meanwhile, the peaks of aromatics such as benzene, methylbenzene, and naphthalene increased significantly. These results indicate that the CPOs could be converted to aromatics at high temperatures, which is consistent with the reports of other reactions[31] or coupling conversions over zeolites.[15] In addition, these CPOs were not detected in the gas-phase effluent by on-line GC, which demonstrates that these CPOs could strongly adsorb on the Brønsted acid sites and undergo further transformation.

Oxygenated polycyclic aromatics containing carbonyl groups were also retained at 500 °C (Figure S5), which indicates that CO could also react with aromatics, leading to more carbon deposition.

3.6. ^{13}C Isotope Tracing Experiments for the Coupling Reaction of *n*-Hexane and CO over HZSM-5. ^{13}C isotope tracing experiments were performed by cofeeding labeled ^{13}CO and unlabeled *n*-hexane at 250 °C. Figure 7 shows the ^{13}C distributions of the CPOs on the catalyst and the aromatics in the gaseous products. The detailed MS spectra are shown in Figures S6 and S7. Most of the CPOs contained one ^{13}C atom, and the observed MS spectra shifted relative to the unlabeled spectra systematically, which indicates that the ^{13}CO molecules participated in the coupling reaction and generated CPOs by incorporating one ^{13}C atom into the intermediates. More interestingly, some of the aromatics in the products contained one ^{13}C atom, whereas other products, such as alkanes and olefins, contained almost no ^{13}C atoms. A detailed analysis of the ion fragmentation patterns in the MS spectra of the aromatics shows that the incorporated ^{13}C atom was located on the aromatic ring, suggesting that some of the aromatics might be generated from CPO intermediates. This route of aromatization is completely different from traditional aromatization via a hydrogen transfer reaction, but it is similar to that reported for a methanol/CO reaction system.[15,31] These experiments clearly reveal that CO was incorporated into the CPOs and was finally transformed into aromatics during the coupling reaction.

3.7. Reaction Mechanism of the Coupling Reaction of *n*-Hexane and CO over HZSM-5. Based on the experimental observations and discussion, a plausible mechanism was proposed for the coupling reaction and is shown in Figure 8. First, *n*-hexane is adsorbed on a Brønsted acid site in HZSM-5 and might form carbonium ions or crack into smaller products. Then, CO adsorbs and inserts into the carbonium ions to generate an acyl group on the acid site. These acyl species adsorbed on the zeolite react with olefins to form important
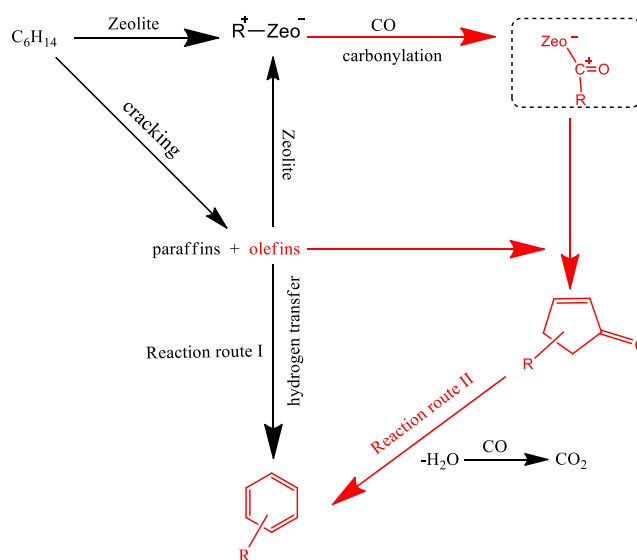

Figure 8. Proposed mechanism for the coupling conversion of *n*-hexane and CO to aromatics over HZSM-5. A new aromatic generation route (reaction route II) and the new intermediates detected experimentally are marked in red.

intermediates, namely, methyl-substituted cyclopentenones (CPOs), by either intramolecular cyclization or coupling with olefins (the latter is known as Friedel−Crafts acylation of alkenes[32]). These CPOs containing 5MR are further transformed into aromatics with 6MR by eliminating one water molecule, leading to improvements in the *n*-hexane conversion and aromatic selectivity of the coupling reaction.[31]

Because olefins easily form carbonium ions over HZSM-5, olefins and CO were cofed in some experiments to further verify the proposed mechanism (Figure 9). Propene (5% C_3H_6 + 95% He) was used in the cofeeding experiments, which were performed at 400 °C. As expected, the aromatic selectivity increased significantly from 43 to 71% and exhibited a nearly linear relationship with the CO partial pressure. Conversely, the alkane selectivity decreased almost linearly. These results are similar to those for the coupling reaction of *n*-hexane and CO, but the effect of the CO partial pressure was more significant for the coupling of propene and CO because it is easier to form carbonium ions from propene over HZSM-5.

In addition, the species retained on the catalysts during the cofeeding of propene and CO were also analyzed by GC−MS (Figure S8). Large numbers of oxygenates containing mainly CPOs were discovered, which is consistent with the results for
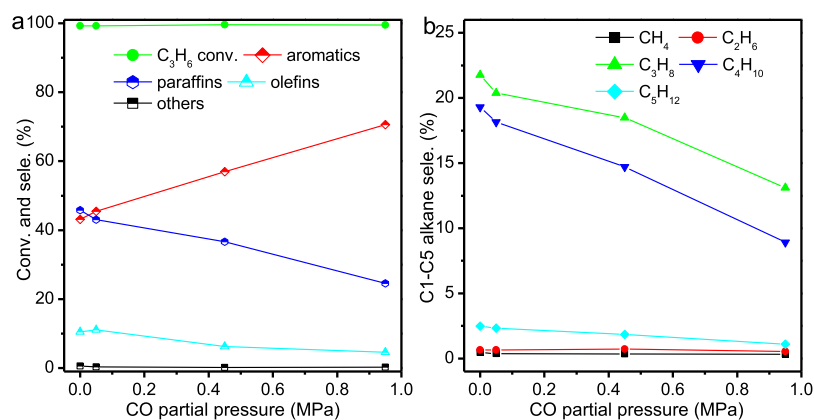
Figure 9. Effects of the CO partial pressure on the coupling reaction of C_3H_6 and CO: (a) conversion and selectivity, (b) C_1-C_5 alkane selectivities. Reaction conditions: T = 400 °C, $WHSV_{C_3H_6}$ = 0.1 $g \cdot g^{-1} h^{-1}$, $P_{(5\%C_3H_6+95\%He)}$ = 0.05 MPa, P_{CO} = 0−0.95 MPa, contact time = 2.1 s.

the coupling of *n*-hexane with CO and further supports the conclusion that the coupling effect for *n*-hexane and CO might work through the reaction of olefins with CO. It was found that the number of CPOs increased significantly with the CO partial pressure, which is consistent with the increase in the aromatic selectivity. These results nicely support the proposed mechanism.

Moreover, CO_2 detected in the coupling conversion might come from the water−gas shift reaction. To verify this hypothesis, a switching experiment was conducted using on-line mass spectrometry to analyze water in the effluent products (Figure S9). The calibration curves for the water content in He and CO atmospheres are shown in Figure S10. The content of water in the *n*-hexane and CO atmosphere ($\sim$2.3 × 10^{-5}, shown in Figure S11) was similar to that calculated using the thermodynamic equilibrium of the water−gas shift reaction ($\sim$9.4 × 10^{-6}, shown in Table S3) and lower than that in the He atmosphere. A ^{13}C isotope tracing experiment indicates that most of the CO_2 molecules in the effluent were $^{13}CO_2$ (Figure S12), which further supports the conclusion that CO_2 was generated from CO by the water−gas shift reaction.

This report is the first to identify both important intermediates and reveal their important roles in the coupling transformation of CO/*n*-hexane, which could alter the H/C balance and account for the high selectivity to aromatics. In addition, this work also demonstrates a new route for aromatic generation, providing new insight into the conversion of alkanes and CO.

4. CONCLUSIONS

The coupling conversion of *n*-hexane with CO over HZSM-5 was systematically studied. It was found that the addition of CO led to a significant increase in the aromatic selectivity and decrease in the alkane selectivity. The CO partial pressure considerably affected the coupling reaction and aromatic selectivity. Increasing the reaction temperature and prolonging the contact time favored aromatic generation. Specifically, an aromatic selectivity of 80% was achieved during the coupling reaction at 500 °C and a CO partial pressure of 3 MPa, far exceeding the theoretical value for the conversion of only *n*-hexane (58%) over HZSM-5. The results of in situ DRIFT characterization, GC−MS analysis and ^{13}C isotope tracing experiments demonstrate that the coupling conversion might proceed by the following reaction route: CO inserts into the

carbonium ions formed from *n*-hexane to generate acyl groups on the Brønsted acid sites, and then the acyl groups couple with olefins to generate oxygenated intermediates (CPOs), which are further transformed into aromatics. Cofeeding propene and CO provided further evidence to support the proposed mechanism. In addition, the coupling conversion of CO and other alkanes such as C_1-C_5 alkanes might also be feasible over acidic zeolite catalysts, which is important for upgrading alkanes and deserves further investigation. Considering the large existing supply capacity of alkanes and CO, this type of coupling reaction might have great potential for industrial applications.

■ ASSOCIATED CONTENT

ⓈI Supporting Information
The Supporting Information is available free of charge at https://pubs.acs.org/doi/10.1021/acscatal.9b05619.

> Additional data regarding the catalyst characterization, catalyst evaluation, MS spectra, and switching experiment (PDF)

■ AUTHOR INFORMATION

Corresponding Author
> **Zhongmin Liu** − *National Engineering Laboratory for Methanol to Olefins, Dalian National Laboratory for Clean Energy, Dalian Institute of Chemical Physics, Chinese Academy of Sciences, Dalian 116023, Liaoning, China;* ⓘ orcid.org/0000-0002-7999-2940; Email: liuzm@dicp.ac.cn

Authors
> **Changcheng Wei** − *National Engineering Laboratory for Methanol to Olefins, Dalian National Laboratory for Clean Energy, Dalian Institute of Chemical Physics, Chinese Academy of Sciences, Dalian 116023, Liaoning, China; University of Chinese Academy of Sciences, Beijing 100049, China*
> **Qijun Yu** − *National Engineering Laboratory for Methanol to Olefins, Dalian National Laboratory for Clean Energy, Dalian Institute of Chemical Physics, Chinese Academy of Sciences, Dalian 116023, Liaoning, China; University of Chinese Academy of Sciences, Beijing 100049, China*
> **Jinzhe Li** − *National Engineering Laboratory for Methanol to Olefins, Dalian National Laboratory for Clean Energy, Dalian Institute of Chemical Physics, Chinese Academy of Sciences, Dalian 116023, Liaoning, China*

Complete contact information is available at:

https://pubs.acs.org/10.1021/acscatal.9b05619

Notes

The authors declare no competing financial interest.

■ REFERENCES

(1) (a) Corma, A.; Melo, F. V.; Sauvanaud, L.; Ortega, F. Light cracked naphtha processing: Controlling chemistry for maximum propylene production. *Catal. Today* **2005**, *107−108*, 699−706. (b) Rahimpour, M. R.; Jafari, M.; Iranshahi, D. Progress in catalytic naphtha reforming process: A review. *Appl. Energy* **2013**, *109*, 79−93.

(2) (a) Bocanegra, S. A.; Castro, A. A.; Guerrero-Ruíz, A.; Scelza, O. A.; de Miguel, S. R. Characteristics of the metallic phase of Pt/Al2O3 and Na-doped Pt/Al2O3 catalysts for light paraffins dehydrogenation. *Chem. Eng. J.* **2006**, *118*, 161−166. (b) Mazzieri, V. A.; Grau, J. M.; Vera, C. R.; Yori, J. C.; Parera, J. M.; Pieck, C. L. Role of Sn in Pt−Re−Sn/Al2O3−Cl catalysts for naphtha reforming. *Catal. Today* **2005**, *107−108*, 643−650.

(3) Tian, P.; Wei, Y.; Ye, M.; Liu, Z. Methanol to olefins (MTO): from fundamentals to commercialization. *ACS Catal.* **2015**, *5*, 1922−1938.

(4) (a) Jiao, F.; Li, J.; Pan, X.; Xiao, J.; Li, H.; Ma, H.; Wei, M.; Pan, Y.; Zhou, Z.; Li, M.; Miao, S.; Li, J.; Zhu, Y.; Xiao, D.; He, T.; Yang, J.; Qi, F.; Fu, Q.; Bao, X. Selective conversion of syngas to light olefins. *Science* **2016**, *351*, 1065−1068. (b) Jiao, F.; Pan, X.; Gong, K.; Chen, Y.; Li, G.; Bao, X. Shape-Selective Zeolites Promote Ethylene Formation from Syngas via a Ketene Intermediate. *Angew. Chem., Int. Ed.* **2018**, *57*, 4692−4696. (c) Cheng, K.; Zhou, W.; Kang, J.; He, S.; Shi, S.; Zhang, Q.; Pan, Y.; Wen, W.; Wang, Y. Bifunctional catalysts for one-step conversion of syngas into aromatics with excellent selectivity and stability. *Chem* **2017**, *3*, 334−347.

(5) (a) Yoneda, N.; Takahashi, Y.; Fukuhara, T.; Suzuki, A. Reaction of Carbocations Derived from Alkanes with Carbon Monoxide in HF−SbF5 Superacid. *Bull. Chem. Soc. Jpn.* **1986**, *59*, 2819−2825. (b) Delavarenne, S.; Simon, M.; Fauconet, M.; Sommer, J. Halogen promoted selective carbonylation of propane in superacid media. *J. Am. Chem. Soc.* **1989**, *111*, 383−384. (c) Farooq, O.; Marcelli, M.; Prakash, G. K. S.; Olah, G. A. Electrophilic reactions at single bonds. 22. Superacid-catalyzed electrophilic formylation of adamantane with carbon monoxide competing with Koch-Haaf carboxylation. *J. Am. Chem. Soc.* **1988**, *110*, 864−867.

(6) Stepanov, A. G.; Luzgin, M. V.; Krasnoslobodtsev, A. V.; Shmachkova, V. P.; Kotsarenko, N. S. Alkane carbonylation with carbon monoxide on sulfated zirconia: NMR observation of ketone and carboxylic acid formation from isobutane and CO. *Angew. Chem.* **2000**, *112*, 3804−3806.

(7) (a) Wang, X.; Qi, G.; Xu, J.; Li, B.; Wang, C.; Deng, F. NMR-Spectroscopic Evidence of Intermediate-Dependent Pathways for Acetic Acid Formation from Methane and Carbon Monoxide over a ZnZSM-5 Zeolite Catalyst. *Angew. Chem.* **2012**, *124*, 3916−3919. (b) Wang, X.; Xu, J.; Qi, G.; Wang, C.; Wang, W.; Gao, P.; Wang, Q.; Liu, X.; Feng, N.; Deng, F. Carbonylation of ethane with carbon monoxide over Zn-modified ZSM-5 zeolites studied by in situ solid-state NMR spectroscopy. *J. Catal.* **2017**, *345*, 228−235.

(8) Luzgin, M. V.; Stepanov, A. G.; Sassi, A.; Sommer, J. Formation of Carboxylic Acids from Small Alkanes in Zeolite H-ZSM-5. *Chem.—Eur. J.* **2000**, *6*, 2368−2376.

(9) Fujimoto, K.; Shikada, T.; Omata, K.; Tominaga, H.-o. Vapor phase carbonylation of methanol with solid acid catalysts. *Chem. Lett.* **1984**, 2047−2050.

(10) Bhan, A.; Allian, A. D.; Sunley, G. J.; Law, D. J.; Iglesia, E. Specificity of sites within eight-membered ring zeolite channels for carbonylation of methyls to acetyls. *J. Am. Chem. Soc.* **2007**, *129*, 4919−4924.

(11) (a) Liu, J.; Xue, H.; Huang, X.; Li, Y.; Shen, W. Dimethyl ether carbonylation to methyl acetate over HZSM-35. *Catal. Lett.* **2010**, *139*, 33−37. (b) Liu, J.; Huifu, X.; Huang, X.; Pei-Hao, W.; Huang, S.-J.; Shang-Bin, L.; Wenjie, S. Stability enhancement of H-mordenite in dimethyl ether carbonylation to methyl acetate by pre-adsorption of pyridine. *Chin. J. Catal.* **2010**, *31*, 729−738.

(12) Celik, F. E.; Kim, T.-J.; Bell, A. T. Vapor-Phase Carbonylation of Dimethoxymethane over H-Faujasite. *Angew. Chem., Int. Ed.* **2009**, *48*, 4813−4815.

(13) Stepanov, A. G.; Luzgin, M. V.; Romannikov, V. N.; Zamaraev, K. I. NMR observation of the koch reaction in zeolite h-zsm-5 under mild conditions. *J. Am. Chem. Soc.* **1995**, *117*, 3615−3616.

(14) Ni, Y.; Shi, L.; Liu, H.; Zhang, W.; Liu, Y.; Zhu, W.; Liu, Z. A green route for methanol carbonylation. *Catal. Sci. Technol.* **2017**, *7*, 4818−4822.

(15) Chen, Z.; Ni, Y.; Zhi, Y.; Wen, F.; Zhou, Z.; Wei, Y.; Zhu, W.; Liu, Z. Coupling of Methanol and Carbon Monoxide over H-ZSM-5 to Form Aromatics. *Angew. Chem., Int. Ed.* **2018**, *57*, 12549−12553.

(16) (a) Primo, A.; Garcia, H. Zeolites as catalysts in oil refining. *Chem. Soc. Rev.* **2014**, *43*, 7548−7561. (b) Siddiqui, M. A. B.; Aitani, A.; Saeed, M.; Al-Khattaf, S. Enhancing the production of light olefins by catalytic cracking of FCC naphtha over mesoporous ZSM-5 catalyst. *Top. Catal.* **2010**, *53*, 1387−1393.

(17) (a) Chang, F.; Wei, Y.; Liu, X.; Zhao, Y.; Xu, L.; Sun, Y.; Zhang, D.; He, Y.; Liu, Z. A mechanistic investigation of the coupled reaction of n -hexane and methanol over HZSM-5. *Appl. Catal., A* **2007**, *328*, 163−173. (b) Chang, F.; Wei, Y.; Liu, X.; Qi, Y.; Zhang, D.; He, Y.; Liu, Z. An Improved Catalytic Cracking of n -hexane via Methanol Coupling Reaction Over HZSM-5 Zeolite Catalysts. *Catal. Lett.* **2006**, *106*, 171−176.

(18) Yang, K.; Li, J.; Zhang, X.; Liu, Z. Investigation of the coupled reaction of methyl acetate and n-hexane over HZSM-5. *Chin. J. Catal.* **2018**, *39*, 1960−1970.

(19) (a) Martin, A.; Nowak, S.; Lücke, B.; Günschel, H. Coupled conversion of methanol and C4 hydrocarbons to lower olefins. *Appl. Catal., A* **1989**, *50*, 149−155. (b) Lücke, B.; Martin, A.; Günschel, H.; Nowak, S. CMHC: coupled methanol hydrocarbon cracking. *Microporous Mesoporous Mater.* **1999**, *29*, 145−157.

(20) (a) Chang, C.; Chen, N.; Koenig, L.; Walsh, D. Synergism in acetic acid/methanol reactions over ZSM-5 zeolites. *Prepr. Pap.—Am. Chem. Soc., Div. Fuel Chem.* **1983**, *28*, 830303. (b) Chen, N. Y.; Walsh, D. E.; Koenig, L. R. Fluidized bed upgrading of wood pyrolysis liquids and related compounds. *Prepr. Pap.—Am. Chem. Soc., Div. Fuel Chem.* **1987**, *32*, 277−289.

(21) (a) Guisnet, M.; Costa, L.; Ribeiro, F. R. Prevention of zeolite deactivation by coking. *J. Mol. Catal. A: Chem.* **2009**, *305*, 69−83. (b) Guisnet, M.; Magnoux, P. Coking and deactivation of zeolites. *Appl. Catal.* **1989**, *54*, 1−27.

(22) (a) Cheung, P.; Bhan, A.; Sunley, G. J.; Iglesia, E. Selective carbonylation of dimethyl ether to methyl acetate catalyzed by acidic zeolites. *Angew. Chem., Int. Ed.* **2006**, *45*, 1617−1620. (b) Cheung, P.; Bhan, A.; Sunley, G.; Law, D.; Iglesia, E. Site requirements and elementary steps in dimethyl ether carbonylation catalyzed by acidic zeolites. *J. Catal.* **2007**, *245*, 110−123.

(23) (a) Zhang, W.; Wang, P.; Yang, C.; Li, C. A Comparative Study of n-Butane Isomerization over H-Beta and H-ZSM-5 Zeolites at Low Temperatures: Effects of Acid Properties and Pore Structures. *Catal. Lett.* **2019**, *149*, 1017−1025. (b) Wang, P.; Wang, S.; Yue, Y.; Wang, T.; Bao, X. Effects of acidity and topology of zeolites on the n-alkane conversion at low reaction temperatures. *Microporous Mesoporous Mater.* **2019**, *292*, 109748.

(24) Celik, F. E.; Kim, T.-J.; Bell, A. T. Effect of zeolite framework type and Si/Al ratio on dimethoxymethane carbonylation. *J. Catal.* **2010**, *270*, 185−195.

(25) van Bokhoven, J. A.; Tromp, M.; Koningsberger, D. C.; Miller, J. T.; Pieterse, J. A. Z.; Lercher, J. A.; Williams, B. A.; Kung, H. H. An explanation for the enhanced activity for light alkane conversion in

mildly steam dealuminated mordenite: The dominant role of adsorption. *J. Catal.* **2001**, *202*, 129−140.

(26) (a) Zhu, N.; Wang, Y.; Cheng, D.-g.; Chen, F.-q.; Zhan, X.-l. Experimental evidence for the enhanced cracking activity of n-heptane over steamed ZSM-5/mordenite composite zeolites. *Appl. Catal., A* **2009**, *362*, 26−33. (b) Kotrel, S.; Rosynek, M. P.; Lunsford, J. H. Origin of First-Order Kinetics during the Bimolecular Cracking of n-Hexane over H-ZSM-5 and H-*β* Zeolites. *J. Catal.* **2000**, *191*, 55−61.

(27) Forester, T. R.; Howe, R. F. In situ FTIR studies of methanol and dimethyl ether in ZSM-5. *J. Am. Chem. Soc.* **1987**, *109*, 5076−5082.

(28) (a) Blasco, T.; Boronat, M.; Concepción, P.; Corma, A.; Law, D.; Vidal-Moya, J. A. Carbonylation of methanol on metal−acid zeolites: evidence for a mechanism involving a multisite active center. *Angew. Chem.* **2007**, *119*, 4012−4015. (b) Luzgin, M.; Thomas, K.; van Gestel, J.; Gilson, J.-P.; Stepanov, A. G. Propane carbonylation on sulfated zirconia catalyst as studied by 13C MAS NMR and FTIR spectroscopy. *J. Catal.* **2004**, *223*, 290−295.

(29) Wei, Y.; Zhang, D.; Liu, Z.; Su, B. Highly efficient catalytic conversion of chloromethane to light olefins over HSAPO-34 as studied by catalytic testing and in situ FTIR. *J. Catal.* **2006**, *238*, 46−57.

(30) Luzgin, M. V.; Stepanov, A. G.; Shmachkova, V. P.; Kotsarenko, N. S. n-Pentane Conversion on Sulfated Zirconia in the Absence and Presence of Carbon Monoxide: Evidence for Monomolecular Mechanism of Isomerization from the 13C MAS NMR Study. *J. Catal.* **2001**, *203*, 273−280.

(31) Liu, Z.; Dong, X.; Liu, X.; Han, Y. Oxygen-containing coke species in zeolite-catalyzed conversion of methanol to hydrocarbons. *Catal. Sci. Technol.* **2016**, *6*, 8157−8165.

(32) Luzgin, M. V.; Romannikov, V. N.; Stepanov, A. G.; Zamaraev, K. I. Interaction of Olefins with Carbon Monoxide on Zeolite H-ZSM-5. NMR Observation of the Friedel-Crafts Acylation of Alkenes at Ambient Temperature. *J. Am. Chem. Soc.* **1996**, *118*, 10890−10891.